Supporting information

Hollow metal-organic framework-based, stimulator of interferon genes pathway-activating nanovaccines for tumor immunotherapy

Yilei Zhao[a], Ruinan Song[a], Zhen Zhang[d], Houyang Hu[a], Wenli Ning[b], Xiuying Duan[a], Jianwei Jiao*[c], Xiao Fu*[b], Guiqiang Zhang*[a, e]

[a] Medical Science and Technology Innovation Center, Shandong First Medical University & Shandong Academy of Medical Sciences, Jinan, Shandong 250117, China.

[b] School of Stomatology, Shandong First Medical University & Shandong Academy of Medical Sciences, Jinan, Shandong 250021, China.

[c] State Key Laboratory of Stem Cell and Reproductive Biology, Institute of Zoology, Chinese Academy of Sciences, Beijing 100101, China.

[d] Jinan Vocational College of nursing, Jinan, Shandong 250102, China.

[e] Shandong Hongkui Medical Laboratory Co., Ltd. Jinan 271100, P. R. China

*To whom correspondence should be addressed:

E-mail: gqzhang2018@163.com; fuxiao@sdfmu.edu.cn; jwjiao@ioz.ac.cn

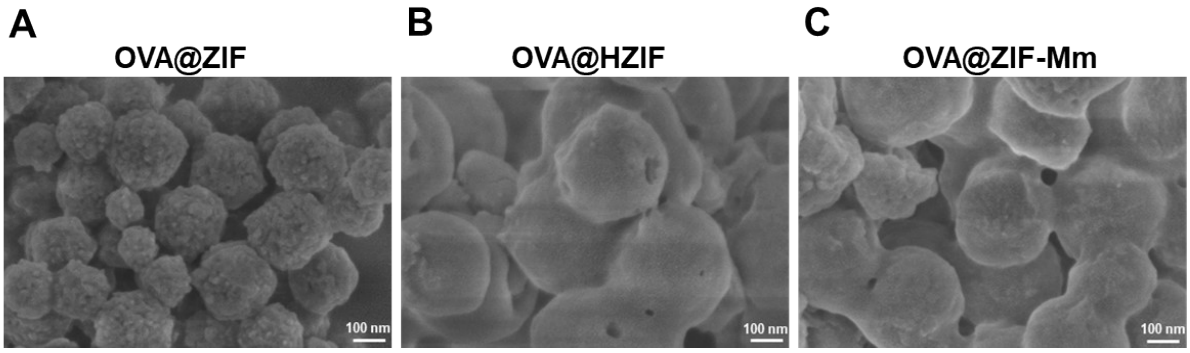

Figure S1. SEM images of OVA@ZIF (A), OVA@HZIF (B) and OVA@HZIF-Mn (C).

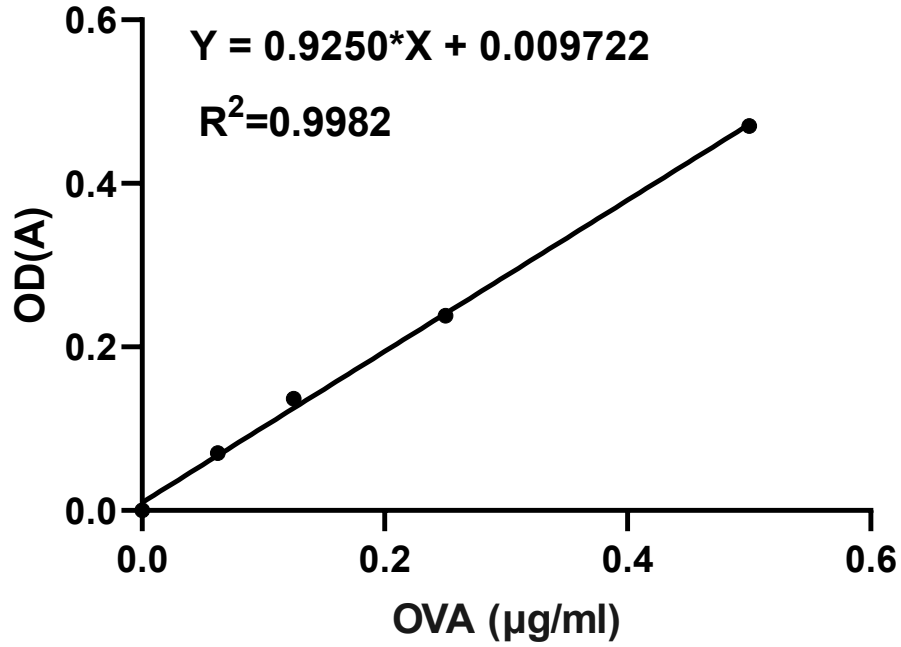

Figure S2. Standard curves of OVA.

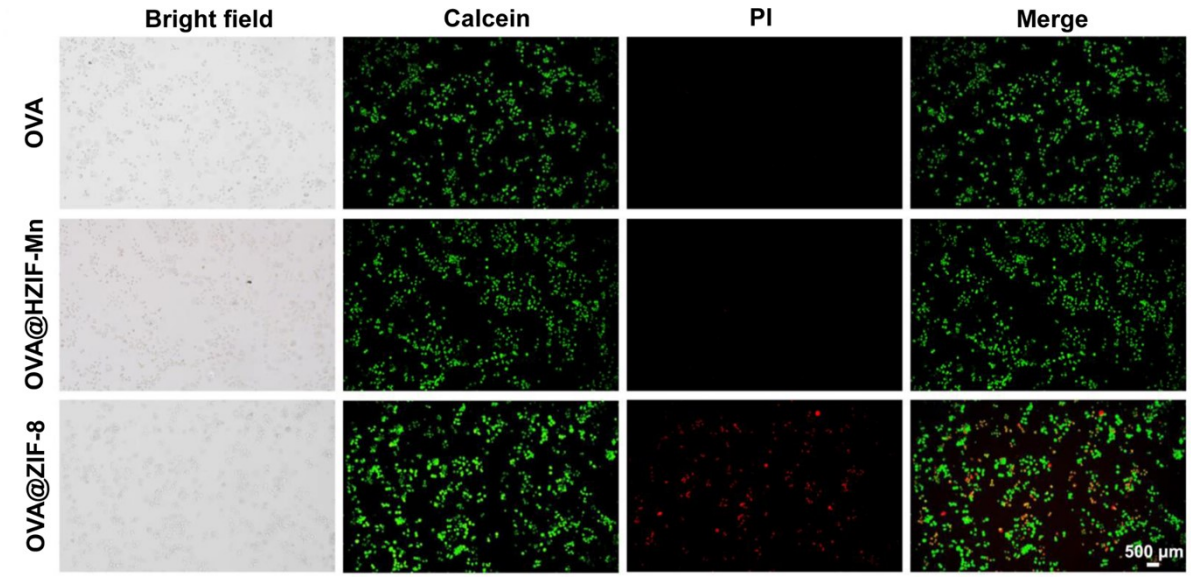

Figure S3. Live/dead analysis with propidium iodide (PI, dead cell, red) and calcein (live cell, green) after various treatments. Scale bars are 500 μm.

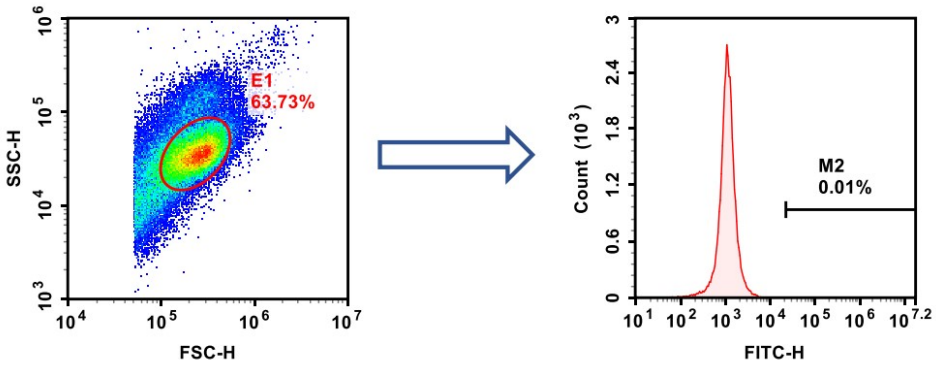

Figure S4. Gating strategy for cellular uptake of OVA and OVA@HZIF-Mn after 4 h incubation. Living cells were identified based on FSC-H versus SSC-H profiles.

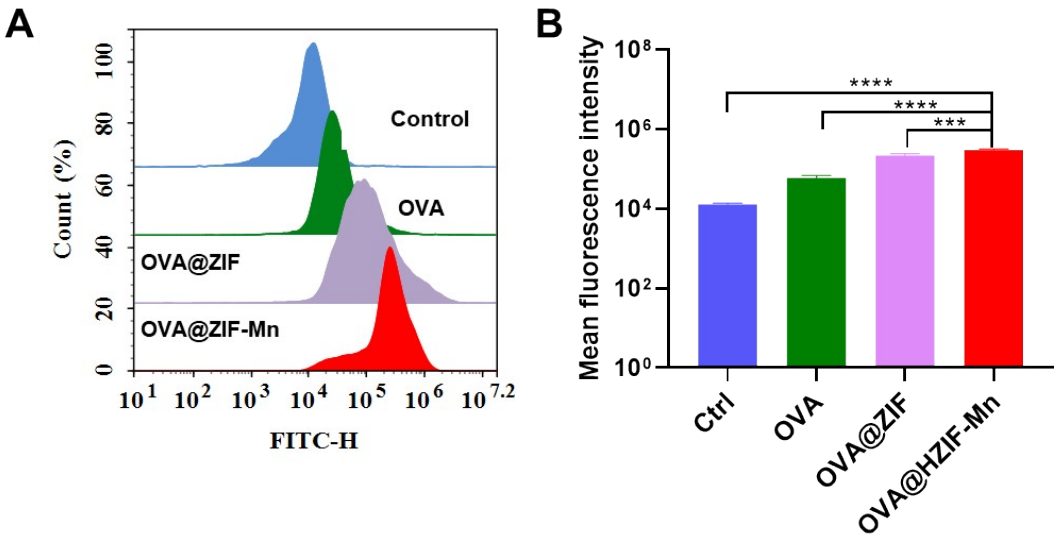

Figure S5. (A) Flow representation and (B) statistics of OVA uptake in DC2.4 cells.

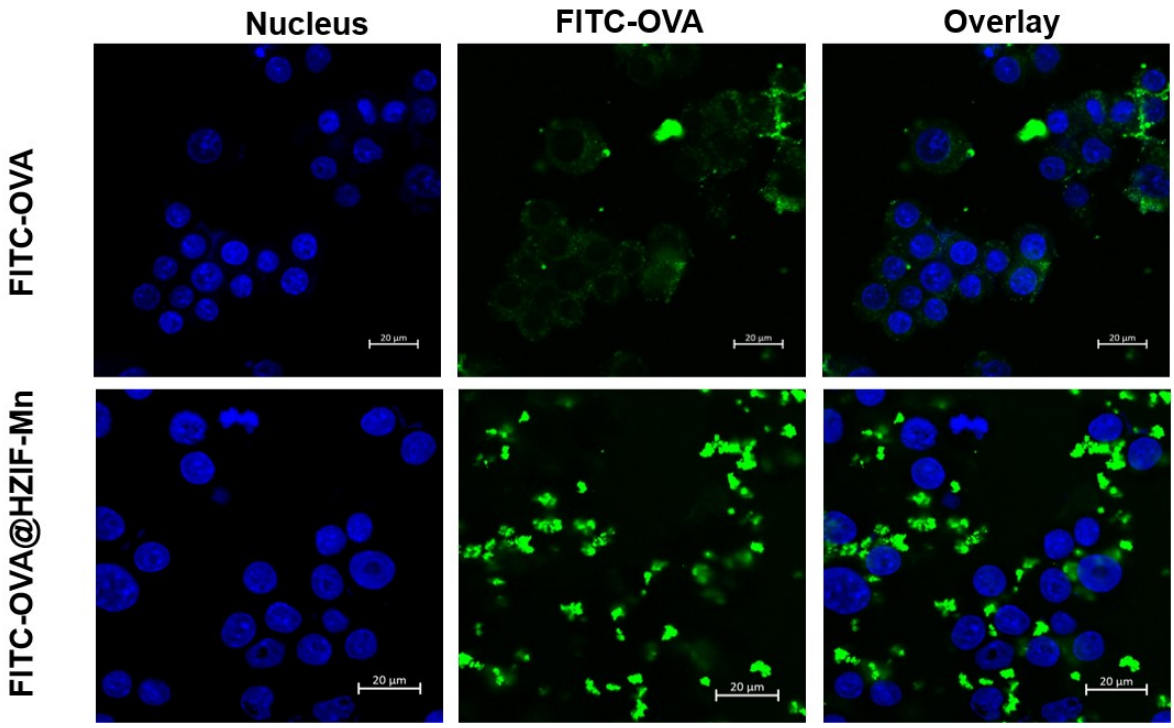

Figure S6. Confocal images of RAW 264.7 treated with FITC-OVA and FITC-OVA@HZIF-Mn for 4 h. The nucleus were stained with DAPI (blue). Scale bars are 20 μm.

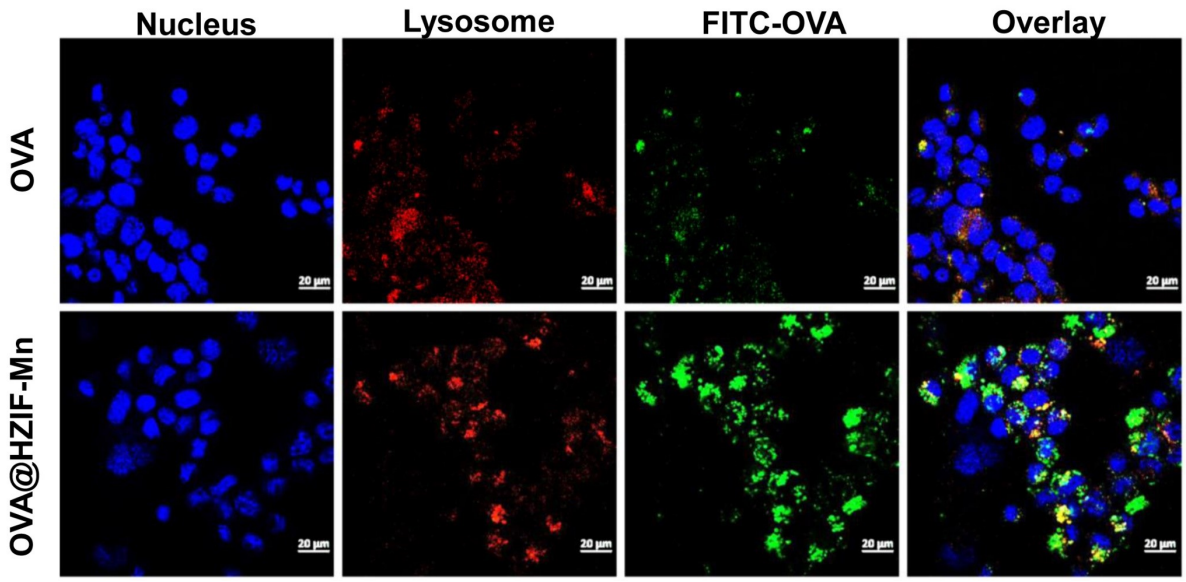

Figure S7. Confocal images of DC2.4 cells treated with FITC-OVA and FITC-OVA@HZIF-Mn to show the lysosome escape of antigen. The nucleus and lysosomes were stained with DAPI (blue) and LysoTracker (red), respectively. Scale bars are 20 μm.

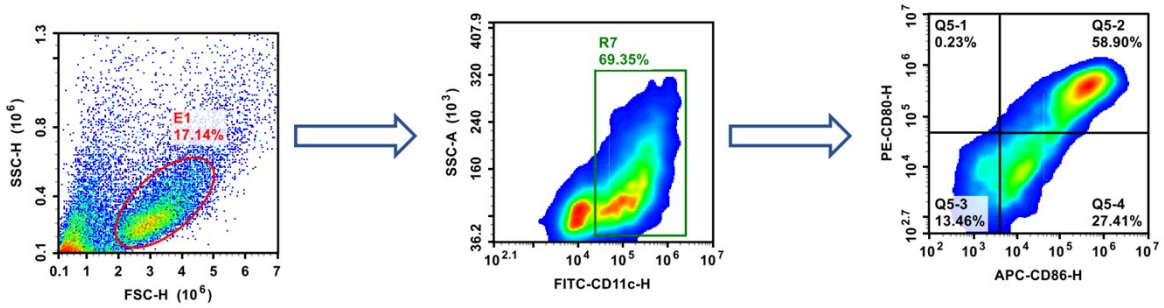

Figure S8. Gating strategy for DC maturation in BMDCs or LNs harvested from the immunized mice. Living cells were identified based on FSC-H versus SSC-H profiles. DCs were identified as $CD11c^{+}$.

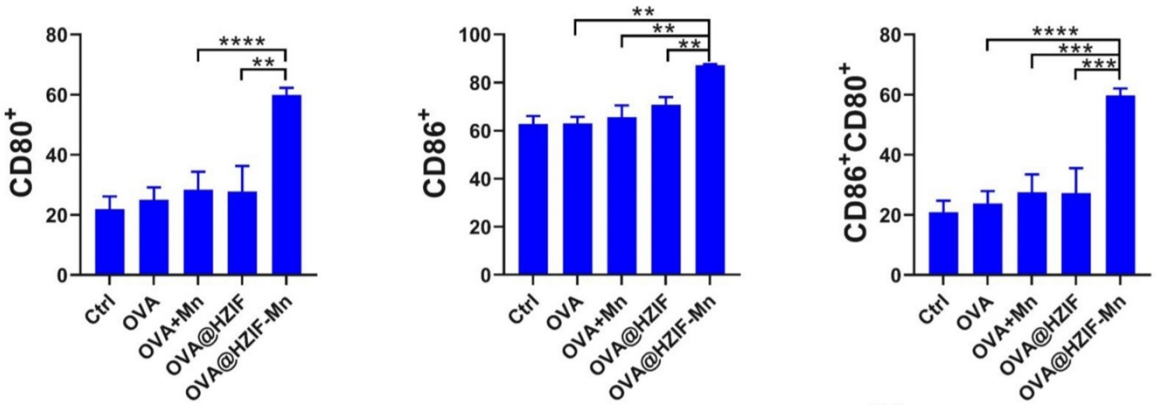

Figure S9. The statistical data of $CD80^+$ (C), $CD86^+$ (D), and $CD80^+CD86^+$ (E) in BMDCs. Data are represented as the mean ± SD (n = 4). $^{**}P < 0.01$, $^{***}P < 0.001$.

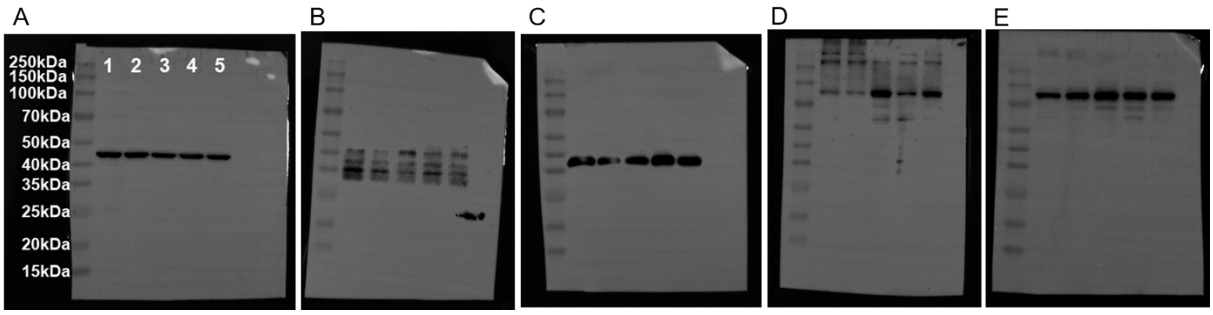

Figure S10. Raw data of western blot of proteins expression of β-actin (A), p-STING (B), STING (C), p-TBK1 (D), and TBK1 (E) after treatment with PBS (1), OVA (2), OVA + Mn (3), OVA@HZIF (4), and OVA@HZIF-Mn (5).

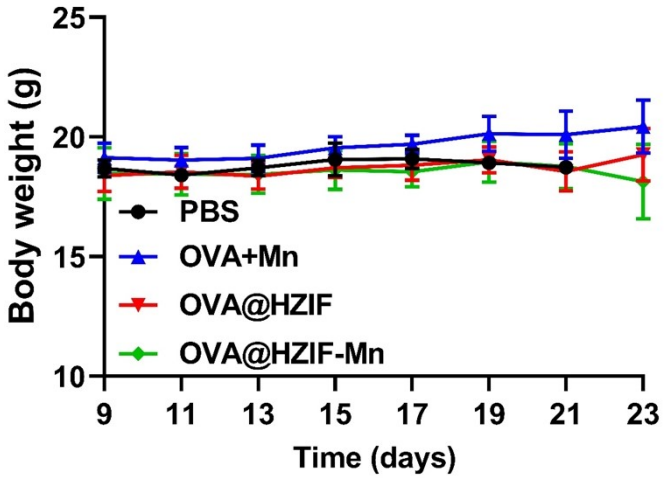

Figure S11. Body weight of mice after various treatments.

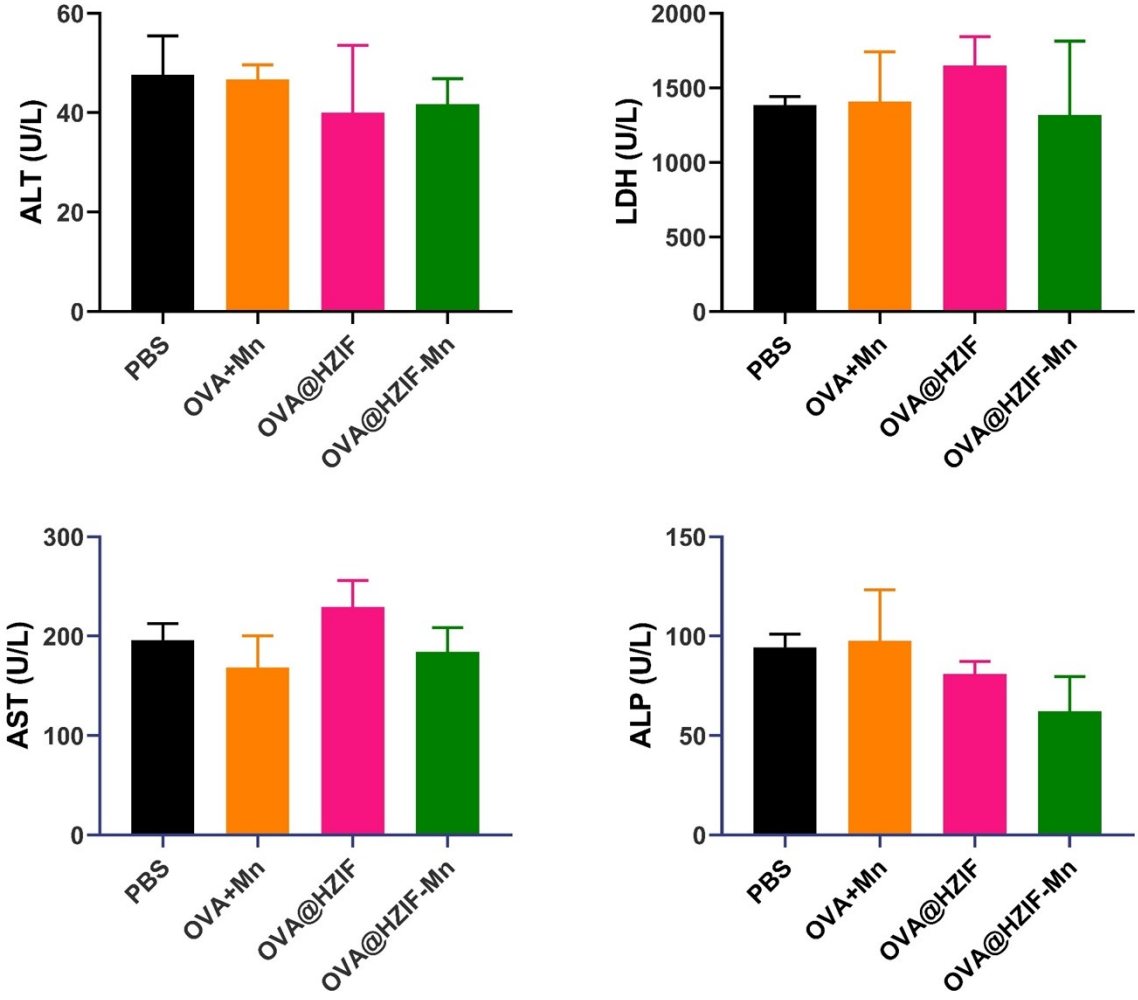

Figure S12. Serum concentration of alanine transaminase (ALT), lactate dehydrogenase (LDH), alkaline phosphatase (ALP) and aspartate transaminase (AST) on day 23 after tumor model establishment. Data are represented as the means ± SD (n=3). $P > 0.05$

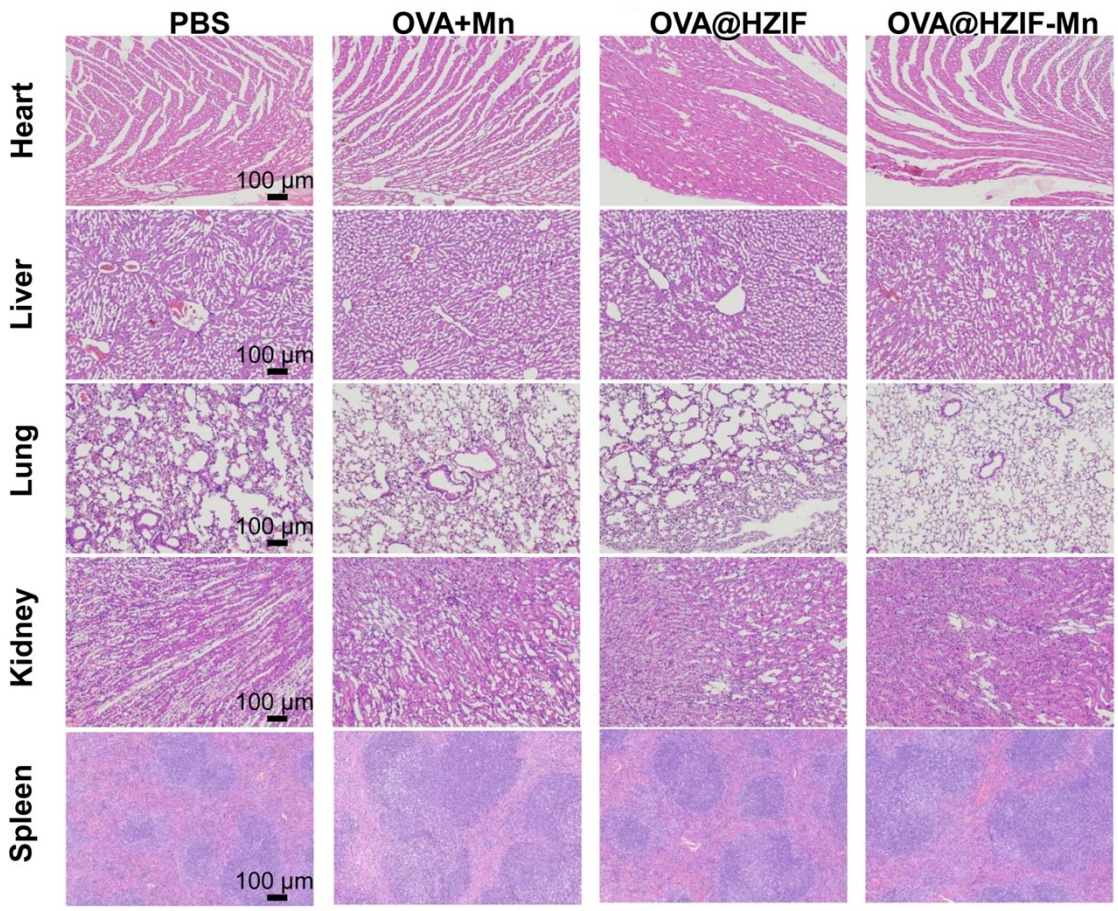

Figure S13. Pathological examination of organs from immunized mice by H&E staining.

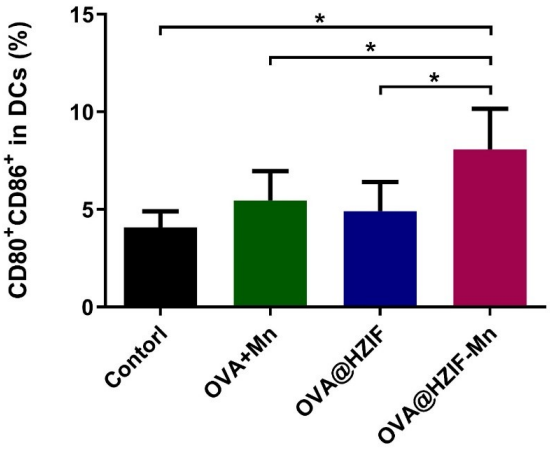

Figure S14. The statistical data of $CD80^+CD86^+$ in BMDCs obtained from LNs. Data are represented as the mean ± SD (n = 6). $^*P < 0.05$.

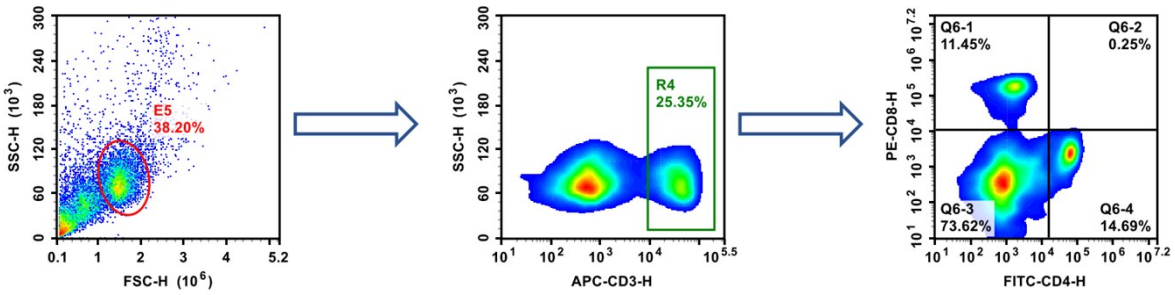

Figure S15. Gating strategy for detection of $CD3^+CD4^+$ and $CD3^+CD8^+$ T cells in LNs harvested from immunized mice. Living cells were identified based on FSC-H versus SSC-H profiles.

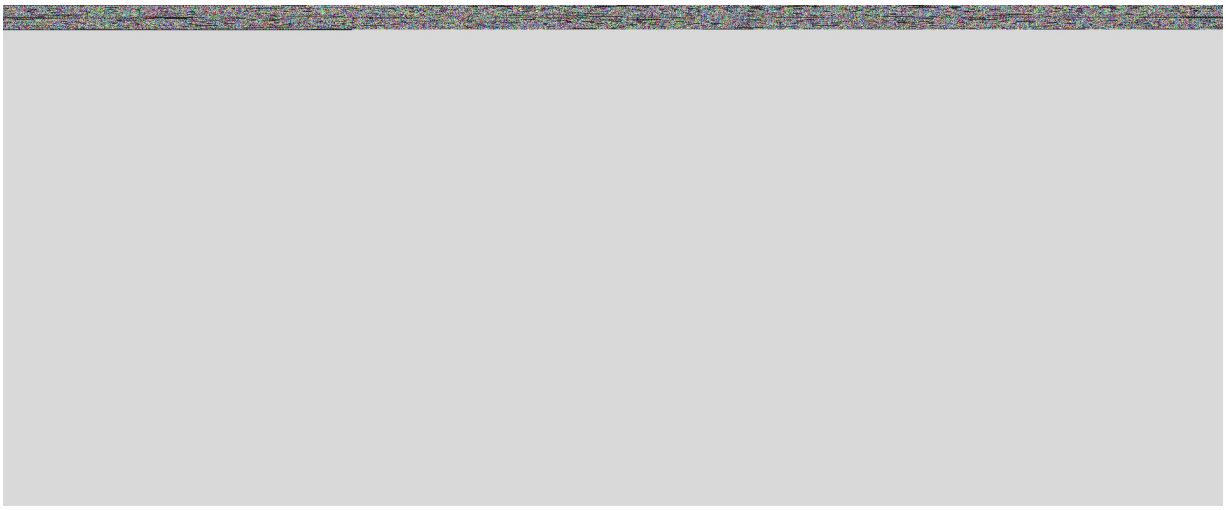

Figure S16. The statistical data of $CD3^+CD8^+$ and $CD3^+CD4^+$ T cells in LNs. Data are represented as the mean ± SD (n = 6). $^{**}P < 0.01$.

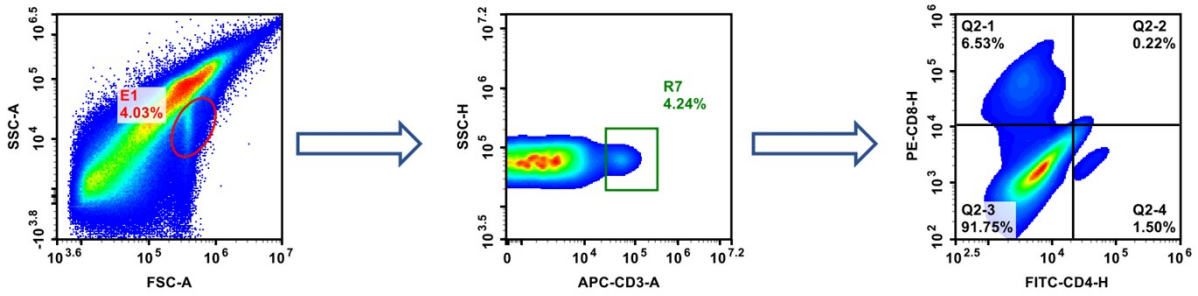

Figure S17. Gating strategy for detection of $CD3^+CD4^+$ and $CD3^+CD8^+$ T cells in tumors harvested from immunized mice. Living cells were identified based on FSC-A versus SSC-A profiles.

Figure S18. The statistical data of $CD3^+CD8^+$, and $CD3^+CD4^+$ T cells in tumors. Data are represented as the mean ± SD (n = 6). $^*P < 0.05$, $^{**}P < 0.01$.

Figure S19. The statistical data of $CD8^+/CD4^+$ in tumors. Data are represented as the mean ± SD (n = 6). $^*P < 0.05$.

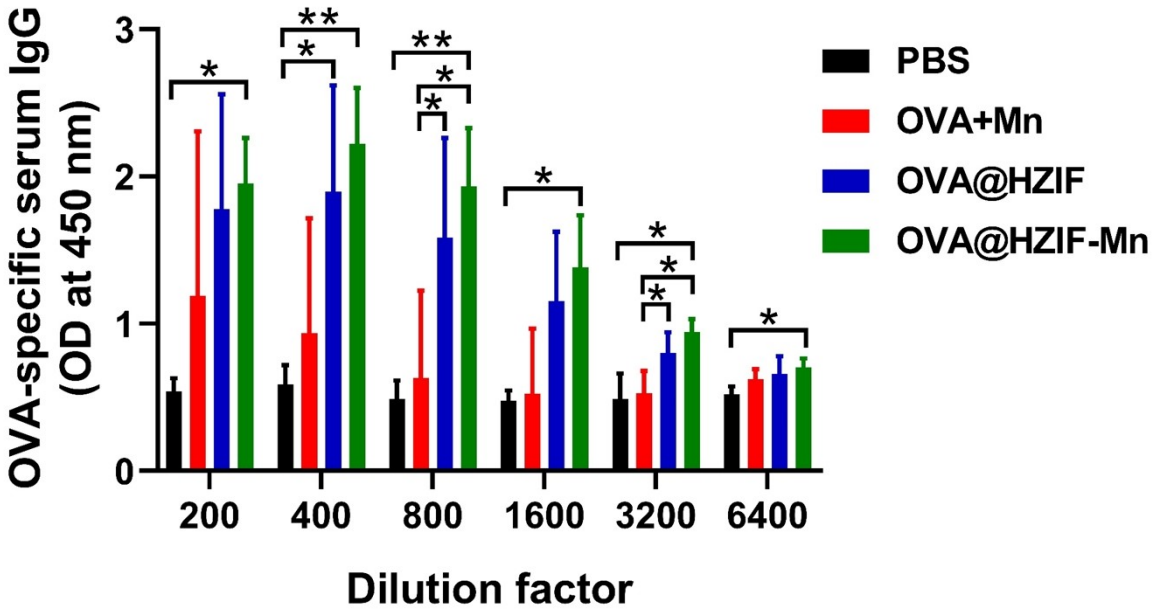

Figure S20. Antigen-specific IgG production in the serum of vaccinated mice. Data are represented as the mean ± SD (n = 6). $^{*}P < 0.05$, $^{**}P < 0.01$.